

Liquid-Crystal Biosensor Based on Nickel-Nanosphere-Induced Homeotropic Alignment for the Amplified Detection of Thrombin

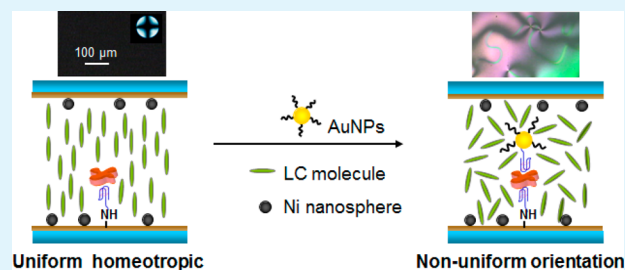
Dongyu Zhao,* Yi Peng, Lihong Xu, Wei Zhou, Qian Wang, and Lin Guo*

School of Chemistry and Environment Science, Beijing University of Aeronautics and Astronautics, Beijing 100191, China

Supporting Information

ABSTRACT: A new liquid-crystal (LC)-based sensor operated by nickel nanosphere (NiNS)-induced homeotropic alignment for the label-free monitoring of thrombin was reported. When doped with NiNSs, a uniform vertical orientation of 4-cyano-4'-pentylbiphenyl (5CB) was easily obtained. A sandwich system of aptamer/thrombin/aptamer-functionalized gold nanoparticles (AuNPs) was fabricated, and AuNPs–aptamer conjugation caused the disruption of the 5CB orientation, leading to an obvious change of the optical appearance from a dark to a bright response to thrombin concentrations from 0.1 to 100 nM. This design also allowed quantitative detection of the thrombin concentration. This distinctive and sensitive thrombin LC sensor provides a new principle for building LC-sensing systems.

KEYWORDS: liquid crystal, thrombin, nickel nanoparticles, biosensor, signal enhancement



Liquid crystals (LCs) are a delicate phase of matter with fluidity, long-range orientational order, and optical anisotropy. Because the anchoring energy of LCs is very low, they are extremely sensitive to external stimuli, and their orientational changes induce different optical appearances. The LC-based sensors amplify and transduce chemical and biological binding events on surfaces into optical outputs visible by the naked eye under crossed polarizers, which permits label-free detection with high sensitivity. Furthermore, the LC-based sensors are portable, avoiding the complex and expensive laboratory-based equipment during the detection procedure. These advantages make LCs particularly attractive in probing DNA,^{1–3} glucose,^{4,5} proteins,^{6,7} lipids,^{8,9} enzymatic activities,^{10–12} and chemical materials including organoamines¹³ and heavy-metal ions.^{14,15} Although LC-based sensing is a convenient probing method, an alignment procedure is still requisite; actually, it is essential for the fabrication of LC sensors.^{2,3,9,14,16–19}

Thrombin is a specific serine protease that plays a significant role in the coagulation cascade and catalyzes many coagulation-related reactions.²⁰ In recent years, different analytical methods were developed for the detection of thrombin, for instance, fluorescence resonant energy transfer,²¹ fluorescence polarization,²² electrochemistry,²³ and plasmonic²⁴ and surface-enhanced resonance scattering.²⁵ Most of them are efficient, sensitive, and specific for the detection of thrombin, but there are still some problems that need to be solved such as the expensiveness of the equipment and the use of fluorescence labels, which are not cheap or toxic (e.g., CdSe). Also, the first attempt using LCs for the detection of thrombin was reported by using of interactions between a polyelectrolyte and a phospholipid monolayer at the aqueous/LC interface.²⁶ Herein,

a new LC-based sensing approach is proposed for the detection of thrombin. We have reported uniform alignment of LCs achieved by dispersing nickel nanomaterials into LCs without an alignment layer.²⁷ In the current strategy, the homeotropic alignment of LCs is simply achieved by doping nickel nanospheres (NiNSs), and the specific interaction between thrombin and its binding aptamers is employed to develop the thrombin LC sensor. Here the disruption to the LC orientation is enhanced by the gold nanoparticles (AuNPs)–aptamer conjugation by utilizing their robust nature, stability, and large surface area and turned to amplification of the optical signals that are directly observed by the naked eye under crossed polarizers. Moreover, we demonstrate quantitative analysis of the thrombin concentrations. Control experiments further confirm the feasibility of this approach. The proposed method is simple, sensitive, and environmentally friendly and does not need expensive equipment, which makes it a promising biosensor for the application of thrombin detection.

In our study, the homeotropic alignment of LCs was first attained by doping NiNSs. After that, the sandwich structure of aptamer/thrombin/aptamer-functionalized AuNPs (Apt-AuNPs) was step-by-step fabricated. All of the experimental details are included in the [Supporting Information](#). The process using the signal amplification of the LC alignment for the detection of thrombin is depicted in [Figure 1](#). First, the surface of the substrate was grafted with (3-glycidioxypropyl)-trimethoxysilane (GPTMS), an epoxy-group-rich compound, to form an epoxysilane monolayer for reacting readily with

Received: September 21, 2015

Accepted: October 12, 2015

Published: October 12, 2015

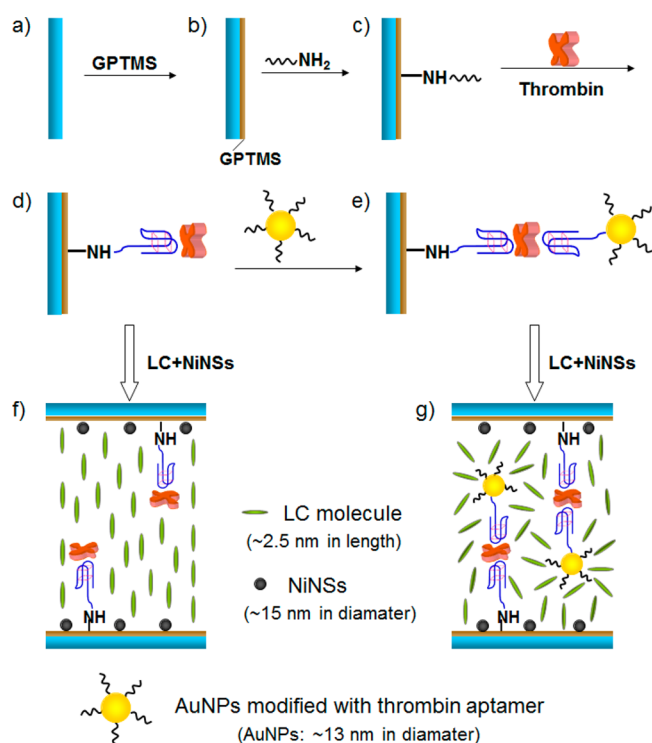


Figure 1. Schematic illustration of the detection method and preparation steps for the NiNS-based thrombin LC sensor: (a) cleaned glass slide; (b) self-assembled GPTMS film; (c) immobilization of the antithrombin aptamer; (d) thrombin addition and binding with the aptamer; (e) binding with Apt-AuNPs; (f) orientation of the LC mixture (SCB doped with 0.01 wt % NiNS) in the LC cells assembled with thrombin; (g) orientation of the LC mixture in the LC cells assembled with Apt-AuNPs through a sandwich format.

amino groups of the aptamers. Then, NH_2 -aptamer was immobilized on the substrate through the coupling reaction between the epoxy and amino groups.²⁸ After that, thrombin was reacted with NH_2 -aptamer with one binding site. Because thrombin includes two binding sites for the aptamer,²⁹ the thrombin molecule is anticipated to act as a bridge to link the monodispersed Apt-AuNPs together to make the aggregation. According to this design, the AuNPs were then reacted with different concentrations of thrombin. Because a single AuNP is loaded with ~ 80 aptamer units per particle,³⁰ these DNA strands will increase the disruption to the LC orientation, resulting in enhancement of the LC optical signals, which can be directly observed by the naked eye under crossed polarizers.

In a current process of a LC biosensor construction, the key step is to fabricate a surface on which the assemble film or the microgroove aligns the LC molecules to a certain orientation. For this purpose, a complicated process to obtain the assemble film or the groove is necessary. Here we use the peculiar characteristic of NiNS-induced vertical alignment of LCs for the detection of thrombin. The alignment of SCB was monitored by polarizing optical microscopy (POM). Before the LC biosensor was assembled, two LC cells filled with SCB and a SCB/NiNSs (Figure S1, Supporting Information) mixture were first assembled. The schlieren texture observed with crossed polarizers in Figure S2a suggested that the nematic LC molecules were randomly oriented. When SCB was doped with NiNSs, a uniform dark image without defects was observed, regardless of the cell rotation angle, as shown in Figure S2b. This result means that the SCB molecules were

oriented perpendicularly to the substrate by doping NiNSs. After determining the vertical anchoring of the LCs, we studied the alignment of this composite in LC cells with an assembled aptamer, as illustrated in Figure 1c. As shown in Figure S2c, the dark image was maintained, indicating that the vertical alignment of the LCs remained after the substrate was assembled with the NH_2 -aptamer. Moreover, a series of LC cells were fabricated with thrombin from low to high density assembled on the surface, and the transitions of the LCs were examined. As shown in Figure S2d–f, when the concentration of thrombin was 1, 10, and 100 nM, the dark image was still observable, indicating that thrombin could not disrupt the perpendicular orientation of the LCs. These results corresponded to the state of Figure 1d. Compared to the conventional LC biosensor, the approach used here did not need the alignment procedure, and as a result, the whole process of detection was greatly simplified.

Because thrombin includes two binding sites for the aptamer, here we use the Apt-AuNPs as the signal disturber for the amplified detection of thrombin. AuNPs (13 ± 1 nm; Figure S3) were first functionalized with the thiolated aptamer, with an average loading of ca. 80 aptamer units per particle. Then the functionalized AuNPs were reacted with different concentrations of thrombin. During this time, thrombin and the Apt-AuNPs were combined by van der Waals forces. This process of AuNP aggregation was monitored by scanning electron microscopy (SEM), as shown in Figure 2. The results showed

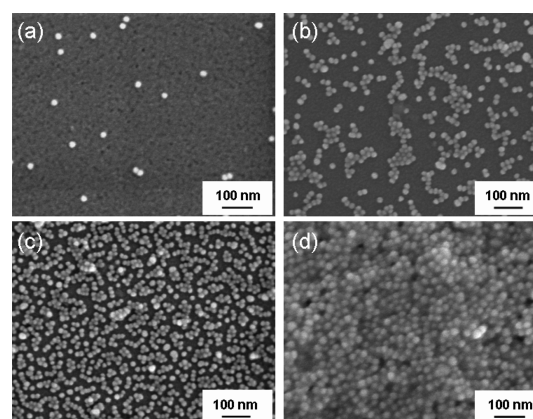


Figure 2. SEM images of indium-tin oxide substrates after AuNP deposition obtained with different concentrations of thrombin: (a) 0.1 nM; (b) 1 nM; (c) 10 nM; (d) 100 nM.

that the amount of Apt-AuNPs increased with an increase of the thrombin concentration, meaning that AuNPs were successfully connected with thrombin. This surface topology change will induce the orientation transition of LC molecules.

To study the POM optical response of AuNPs-aptamer conjugation without thrombin, the NH_2 -aptamer-aptamer substrates were dipped into an AuNPs-aptamer solution to fabricate the proposed LC cell. As shown in Figure S4, the changed dark image of POM indicates that the LC biosensor has no response to the AuNPs-aptamer. Obviously, this result is due to no immobilization of the AuNPs-aptamer on the substrate without thrombin as the linkage to form the aptamer/thrombin/AuNPs-aptamer sandwich structure.

The loading of aptamers on the AuNP surface was also performed to study the transition of the LC orientation. As shown in Figure S5a, LCs are oriented perpendicularly without

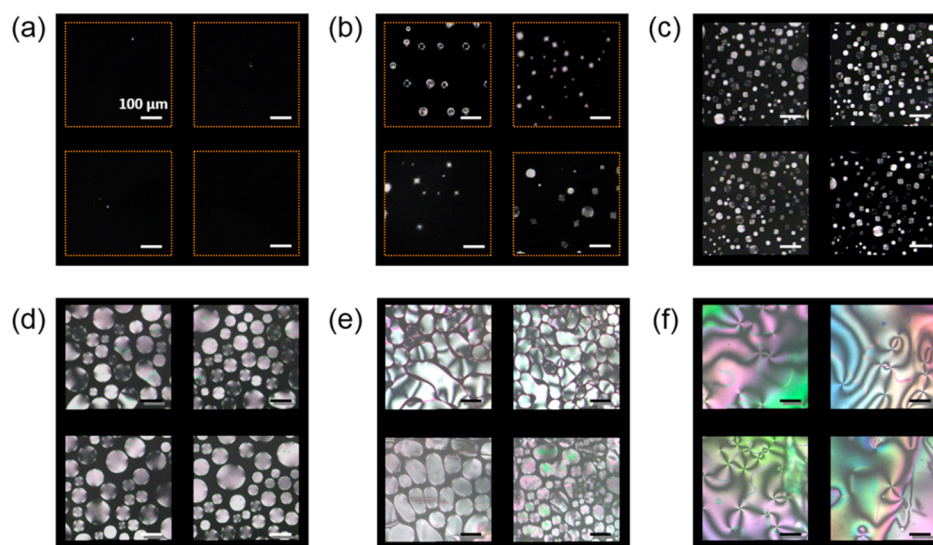


Figure 3. POM images of 5CB doped with 0.01 wt % NiNSs in LC cells with substrates assembled with thrombin and the functionalized AuNPs. Thrombin is at concentrations of (a) 0.0, (b) 0.1, (c) 1, (d) 10, (e) 50, and (f) 100 nM. The scale bars in all panels are 100 μm .

any aptamers, which suggested that the bare AuNPs have no contribution to LCs' orientation changes. Parts b–d of Figure S5 exhibited the POM images of the LC cells tested with increasing aptamer loading; interestingly, the LC orientation was disturbed more intensively, which strongly suggested that the LC reorientation was contributed by the aptamer loading on the AuNP surface.

After aggregation of the AuNPs, a series of LC cells were assembled, and the detection of thrombin was observed with POM. Figure 3 shows the optical textures of 5CB in contact with surfaces on which the functionalized AuNPs were reacted with different concentrations of thrombin. In order to demonstrate the repeatability and reproducibility of this method, every thrombin concentration is shown by four photographs in Figure 3. When the target thrombin is over 0.1 nM, some bright spots start to form over the dark image, suggesting that the homeotropic alignment is disrupted because of the strand-like aptamers and some tilt or planar domains start to form. With the concentration of thrombin increased from 0.1 to 50 nM, it can be observed that the bright domains expand increasingly, meaning that the amount of AuNPs increased with an increase in the target thrombin, as shown in Figure 3b–e. Therefore, the orientation signals of LCs are disturbed increasingly, and the region of vertical orientation is decreased more and more. When the concentration of thrombin reaches to 100 nM, the disruption is the most intensive, and the homeotropic orientation of the LC molecules disappears completely, as shown in Figure 3f.

Because the area of bright LC regions increased with increasing thrombin concentration, we tried to investigate the correlation between the concentration of thrombin and the intensity of the LC optical signal quantitatively. Through measurement of the area ratio of the bright LC regions to the whole image with computer software, quantitative analysis of the thrombin concentration was achieved. As shown in Figure 4, the ratio keeps rising with an increase of the thrombin concentration. The rate of the bright area enhancement is fast at low thrombin concentrations and becomes slower at high thrombin concentrations. The detection limit is as low as 0.06 nM. In the thrombin concentration range of 0.1–1.0 nM, the

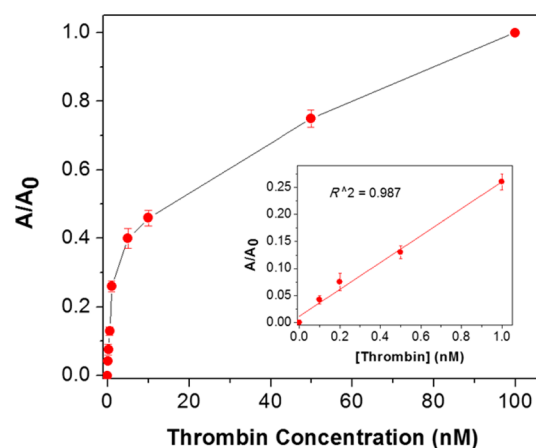


Figure 4. Correlations between the area ratio of the bright LC regions to the whole image and the concentration of thrombin. Inset: Linear relationship between the area ratio and the thrombin concentration. A = area of the bright LC regions. A_0 = area of the whole image. The illustrated error bars represent the standard deviation of four measurements of a sample for each assay.

plot of ratio A/A_0 as a function of the thrombin concentration is a linear line with a high correlation coefficient (0.987).

Several control experiments were performed to demonstrate the specificity of the LC aptasensor, determined by challenging it with nonspecific aptamers and nontargeted proteins. First, the LC response upon the addition of a nonspecific aptamer (aptamer 3) containing mismatch bases to the assembled surface was tested. It was found that the POM image was still dark under cross polarizers, meaning that the homeotropic LC orientation was maintained (Figure S6a). Moreover, the LC optical signal upon the use of similar proteins, including 10 nM bovine hemoglobin, 10 nM bovine serum albumin, and 10 nM lysozyme, in the LC sensing system was investigated, as shown in Figure S6b–d. In these control experiments, no LC reorientation was observed. We inferred that the proteins had no specific binding to the antithrombin aptamer; thus, no aggregation occurred. To further investigate this point, we studied the LC response with mixtures containing thrombin and these different proteins. As shown in Figure S7, the POM

image exhibits a uniform dark field in the absence of thrombin (Figure S7a,e,i). However, when we added 1 nM thrombin, the birefringence dots obviously emerged (Figure S7b,f,j). When thrombin was added to 50 nM (Figure S7d,h,i), the birefringence regions increased dramatically, indicating vertical anchoring of the LCs was disrupted sharply. This excellent selectivity arises from the high specificity of the antithrombin aptamer.

In summary, we demonstrated a novel approach for the detection of thrombin by using LCs doped with NiNSs. The homeotropic orientation of 5CB molecules was easily obtained by the doped NiNSs. The Apt-AuNPs were aggregated on the substrate surface because thrombin includes two binding sites for the aptamer, and this aggregation made the strandlike aptamers amplify the disruption of the LC orientation. As a result, the LCs underwent an orientation transition, which was easily visualized, so that thrombin with concentrations of 0.1–100 nM was detected. We show that the assay can detect thrombin with high specificity. Moreover, the thrombin concentration could be determined quantitatively, through the ratio of area of the bright LC region to the whole image, thanks to the unique birefringent properties of LCs. This process of detecting thrombin represents a simplified path and has potential application in the fabrication of convenient LC sensors.

■ ASSOCIATED CONTENT

Supporting Information

The Supporting Information is available free of charge on the ACS Publications website at DOI: 10.1021/acsami.5b08924.

Experimental section, TEM images of NiNSs, AuNPs, and results of the control experiments (PDF)

■ AUTHOR INFORMATION

Corresponding Authors

*E-mail: zhaodongyu@buaa.edu.cn.

*E-mail: guolin@buaa.edu.cn.

Notes

The authors declare no competing financial interest.

■ ACKNOWLEDGMENTS

This work was supported by the National Natural Science Foundation of China (Grant 51203005), the New Teacher Fund for Doctor Station, the Ministry of Education of China (Grant 20121102120045), and the Fundamental Research Funds for the Central Universities of China.

■ REFERENCES

- (1) Lai, S. L.; Yang, K. L. Detecting DNA Targets through the Formation of DNA/CTAB Complex and Its Interactions with Liquid Crystals. *Analyst* **2011**, *136*, 3329–3334.
- (2) Tan, H.; Yang, S. Y.; Shen, G. L.; Yu, R. Q.; Wu, Z. Y. Signal-Enhanced Liquid-Crystal DNA Biosensors Based on Enzymatic Metal Deposition. *Angew. Chem., Int. Ed.* **2010**, *49*, 8608–8611.
- (3) Price, A. D.; Schwartz, D. K. DNA Hybridization-Induced Reorientation of Liquid Crystal Anchoring at the Nematic Liquid Crystal/Aqueous Interface. *J. Am. Chem. Soc.* **2008**, *130*, 8188–8194.
- (4) Khan, M.; Park, S. Y. Liquid Crystal-based Proton Sensitive Glucose Biosensor. *Anal. Chem.* **2014**, *86*, 1493–1501.
- (5) Zhong, S.; Jang, C. H. Highly Sensitive and Selective Glucose Sensor Based on Ultraviolet-treated Nematic Liquid Crystals. *Biosens. Bioelectron.* **2014**, *59*, 293–299.
- (6) Gupta, V. K.; Skaife, J. J.; Dubrovsky, T. B.; Abbott, N. L. Optical Amplification of Ligand-Receptor Binding Using Liquid Crystals. *Science* **1998**, *279*, 2077–2080.
- (7) Aliño, V. J.; Sim, P. H.; Choy, W. T.; Fraser, A.; Yang, K. L. Detecting Proteins in Microfluidic Channels Decorated with Liquid Crystal Sensing Dots. *Langmuir* **2012**, *28*, 17571–17577.
- (8) Brake, J. M.; Daschner, M. K.; Luk, Y. Y.; Abbott, N. L. Biomolecular Interactions at Phospholipid-Decorated Surfaces of Liquid Crystals. *Science* **2003**, *302*, 2094–2097.
- (9) Hartono, D.; Qin, W. J.; Yang, K. L.; Yung, L. Y. L. Imaging the Disruption of Phospholipid Monolayer by Protein-coated Nanoparticles Using Ordering Transitions of Liquid Crystals. *Biomaterials* **2009**, *30*, 843–849.
- (10) Hu, Q. Z.; Jang, C. H. Imaging Trypsin Activity through Changes in the Orientation of Liquid Crystals Coupled to the Interactions Between a Polyelectrolyte and A Phospholipid Layer. *ACS Appl. Mater. Interfaces* **2012**, *4*, 1791–1795.
- (11) Liao, S. Z.; Qiao, Y. N.; Han, W. T.; Xie, Z. X.; Wu, Z. Y.; Shen, G. L.; Yu, R. Q. Acetylcholinesterase Liquid Crystal Biosensor Based on Modulated Growth of Gold Nanoparticles for Amplified Detection of Acetylcholine and Inhibitor. *Anal. Chem.* **2012**, *84*, 45–49.
- (12) Bi, X. Y.; Hartono, D.; Yang, K. L. Real-Time Liquid Crystal pH Sensor for Monitoring Enzymatic Activities of Penicillinase. *Adv. Funct. Mater.* **2009**, *19*, 3760–3765.
- (13) Shah, R. R.; Abbott, N. L. Orientational Transitions of Liquid Crystals Driven by Binding of Organoamines to Carboxylic Acids Presented at Surfaces with Nanometer-Scale Topography. *Langmuir* **2003**, *19*, 275–284.
- (14) Yang, S. Y.; Wu, C.; Tan, H.; Wu, Y.; Liao, S. Z.; Wu, Z. Y.; Shen, G. L.; Yu, R. Q. Label-Free Liquid Crystal Biosensor Based on Specific Oligonucleotide Probes for Heavy Metal Ions. *Anal. Chem.* **2013**, *85*, 14–18.
- (15) Hu, Q. Z.; Jang, C. H. Liquid Crystal-based Sensors for the Detection of Heavy Metals Using Surface-immobilized Urease. *Colloids Surf., B* **2011**, *88*, 622–626.
- (16) Xu, H.; Bi, X. Y.; Ngo, X.; Yang, K.-L. Principles of Detecting Vaporious Thiols Using Liquid Crystals and Metal Ion Microarrays. *Analyst* **2009**, *134*, 911–915.
- (17) Van Nelson, J. A.; Kim, S. R.; Abbott, N. L. Amplification of Specific Binding Events Between Biological Species Using Lyotropic Liquid Crystals. *Langmuir* **2002**, *18*, 5031–5035.
- (18) Malone, S. M.; Schwartz, D. K. Macroscopic Liquid Crystal Response to Isolated DNA Helices. *Langmuir* **2011**, *27*, 11767–11772.
- (19) Tyagi, M.; Chandran, A.; Joshi, T.; Prakash, J.; Agrawal, V. V.; Biradar, A. M. Self-Assembled Monolayer Based Liquid Crystal Biosensor for Free Cholesterol Detection. *Appl. Phys. Lett.* **2014**, *104*, 154104.
- (20) Ji, J.; Gan, J. R.; Kong, J. L.; Yang, P. Y.; Liu, B. H.; Ji, C. Electrochemical Detection of the Activities of Thrombin and Its Inhibitor. *Electrochem. Commun.* **2012**, *16*, 53–56.
- (21) Chen, H. Q.; Yuan, F.; Wang, S. Z.; Xu, J.; Zhang, Y. Y.; Wang, L. Aptamer-based Sensing for Thrombin in Red Region via Fluorescence Resonant Energy Transfer Between NaYF₄:Yb,Er Upconversion Nanoparticles And Gold Nanorods. *Biosens. Bioelectron.* **2013**, *48*, 19–25.
- (22) Yue, Q. L.; Shen, T. F.; Wang, L.; Xu, S. L.; Li, H. B.; Xue, Q. W.; Zhang, Y. F.; Gu, X. H.; Zhang, S. Q.; Liu, J. F. A Convenient Sandwich Assay of Thrombin in Biological Media Using Nanoparticle-enhanced Fluorescence Polarization. *Biosens. Bioelectron.* **2014**, *56*, 231–236.
- (23) Zhang, Z.; Luo, L. Q.; Zhu, L. M.; Ding, Y. P.; Deng, D. M.; Wang, Z. X. Aptamer-linked Biosensor for Thrombin Based on AuNPs/thionine-graphene Nanocomposite. *Analyst* **2013**, *138*, 5365–5370.
- (24) Yan, J.; Wang, L. D.; Tang, L. H.; Lin, L.; Liu, Y.; Li, J. H. Enzyme-guided Plasmonic Biosensor Based on Dual-functional Nanohybrid for Sensitive Detection of Thrombin. *Biosens. Bioelectron.* **2015**, *70*, 404–410.

(25) Li, X. M.; Wang, L. L.; Li, C. X. Rolling-Circle Amplification Detection of Thrombin Using Surface-Enhanced Raman Spectroscopy with Core-Shell Nanoparticle Probe. *Chem. - Eur. J.* **2015**, *21*, 6817–6822.

(26) Zhang, M.; Jang, C. H. Liquid Crystal-based Detection of Thrombin Couple to Interactions Between A Polyelectrolyte And A phospholipid Monolayer. *Anal. Biochem.* **2014**, *455*, 13–19.

(27) Zhao, D. Y.; Zhou, W.; Cui, X. P.; Tian, Y.; Guo, L.; Yang, H. Alignment of Liquid Crystals Doped with Nickel Nanoparticles Containing Different Morphologies. *Adv. Mater.* **2011**, *23*, 5779–5784.

(28) Dong, H. F.; Yan, F.; Ji, H. X.; Wong, D. K. Y.; Ju, H. X. Quantum-Dot-Functionalized Poly(styrene-co-acrylic acid) Microbeads: Step-Wise Self-Assembly, Characterization, and Applications for Sub-femtomolar Electrochemical Detection of DNA Hybridization. *Adv. Funct. Mater.* **2010**, *20*, 1173–1179.

(29) Bock, L. C.; Griffin, L. C.; Latham, J. A.; Vermaas, E. H.; Toole, J. J. Selection of Single-stranded DNA Molecules That Bind And Inhibit Human Thrombin. *Nature* **1992**, *355*, 564–566.

(30) Pavlov, V.; Xiao, Y.; Shlyahovsky, B.; Willner, I. Aptamer-Functionalized Au Nanoparticles for the Amplified Optical Detection of Thrombin. *J. Am. Chem. Soc.* **2004**, *126*, 11768–11769.